coatings

MDPI

Article

High-Performance Adhesives Based on Maleic Anhydride-g-EPDM Rubbers and Polybutene for Laminating Cast Polypropylene Film and Aluminum Foil

Sang-Hyub Lee [1], Se-Woo Yang [2], Eun-Suk Park [2], Ji-Young Hwang [2] and Dai-Soo Lee [1,*]

[1] Division of Semiconductor and Chemical Engineering, Chonbuk National University, 567 Baekjedaero, Jeonju 54896, Korea; shlee87@jbnu.ac.kr

[2] LG Chem R & D Campus, 188 Moonji-ro, Yuseong-gu, Daejeon 34122, Korea; swyangc@lgchem.com (S.-W.Y.); fastmover@lgchem.com (E.-S.P.); jiyoungh@lgchem.com (J.-Y.H.)

* Correspondence: daisoolee@jbnu.ac.kr; Tel.: +82-63-270-2431

Received: 30 November 2018; Accepted: 16 January 2019; Published: 21 January 2019

Abstract: The adhesion between aluminum (Al) foil and cast polypropylene (CPP) film laminated with mixtures of amorphous- and crystalline-maleic anhydride-grafted ethylene-propylene-diene monomer (MAH-g-EPDM) rubbers and highly reactive polybutene (HRPB) as the adhesives was investigated. Specifically, the HRPB was used as an adhesion promoter of the MAH-g-EPDM rubbers and CPP as well as a compatibilizer of two kinds of MAH-g-EPDM rubbers having limited miscibility. To introduce strong chemical bonds between the MAH-g-EPDM rubbers and Al foil, the surface of Al foil was treated with 3-aminopropyl triethoxysilane (APTES). The weak adhesion between Al foil and MAH-g-EPDM rubbers was improved by imidization between the amine groups ($–NH_2$) of APTES and the maleic anhydride groups (MAH) of MAH-g-EPDM rubbers. The effects of the composition of adhesives, tempering time and adhesive thickness were also studied to optimize the adhesion of the CPP/Al foil laminates. We concluded that MAH-g-EPDM rubber based adhesives containing HRPB can be applied for the lamination of Al foil and CPP films to satisfy the requirements of high-performance packaging materials for various purposes.

Keywords: maleic anhydride-grafted ethylene-propylene-diene monomer (MAH-g-EPDM) rubber; highly reactive polybutene; silane coupling agent; imidization

1. Introduction

Aluminum (Al) foils are widely used as protective materials in coating and packaging in electronic devices because of their resistance against air and moisture [1–5]. However, poor mechanical properties of Al foil make it prone to tearing, greatly limiting its application. Therefore, the lamination of Al foils with polymer films such as polypropylene (PP) and polyethylene (PE) have been investigated to enhance their performance. The laminated polymers efficiently protect the Al surface from damages that decrease the protective ability of the Al foil [6–15]. In particular, such polymer-based Al-foil laminates have been studied as a soft packaging material for lithium-ion batteries. These polymer-based Al-foil laminates are more suitable in terms of price, weight and heat dissipation compared to the conventional metal containers used for the packaging of lithium-ion batteries [1,14,15]. In this study, cast polypropylene (CPP) film was investigated as a protective material for the Al foil. To obtain a CPP-laminated Al foil with high durability, it is critical to achieve strong interfacial adhesion between the polymer layers and Al foil. Resins derived from polyurethane (PU) and epoxy resin (EP) have been widely used as adhesives as well as coating materials [8–15], which can be suitable candidates

for such adhesion. However, the high polarity of PU and EP make them unsuitable for use in highly polar or high-pH conditions. Thus, PP- or PE-containing adhesives with excellent chemical resistance and similar polarity to CPP could be better choices for laminating films of CPP and Al foil. Liang et al. reported that PP grafted with glycidyl methacrylate, acrylic acid or maleic anhydride improved its adhesion strength with the treated Al foil in the T-peel test [16]. However, generally the high crystallinity [17–20] and non-polarity [21] of PE and PP make it difficult to obtain homogeneous coatings on Al foil and negatively affect its processability.

Ethylene-propylene-diene monomer (EPDM) rubber is a versatile polymer based on copolymer of ethylene and propylene backbone and it has been widely used as an elastomer in automotive parts, sports goods and packaging materials because of its excellent chemical inertness and physical properties. EPDM rubber also shows high resistance to heat, oxidation and ozone, resulting in excellent weatherability [22–29]. Despite its excellent performances, EPDM rubber is relatively non-polar and shows limited compatibility with other materials and solvents. To adjust its polarity and expand its range of application, many attempts have been made to chemically graft the EPDM backbone with maleic anhydride (MAH) [30–38]. The MAH-g-EPDM rubber has received considerable attention because introducing the MAH group onto the non-polar EPDM backbone greatly changes the polarity of EPDM rubber along with its compatibility with other materials; further, the introduction of MAH also allows EPDM rubber to react with other chemicals containing isocyanate (N=C=O) or amine (–NH) groups [39–46]. MAH-g-EPDM rubber shows reasonable compatibility with CPP and its reactive MAH group is expected to result in strong adhesion between surface-treated Al foil and CPP film; thus, MAH-g-EPDM rubber was chosen as the adhesive between Al foil and CPP in this study. To the best of our knowledge, there was no report in literatures based on EPDM rubber for the lamination of Al foil and CPP film. To ensure the toughness and ductility of MAH-g-EPDM-rubber-based adhesives, two types of MAH-g-EPDM rubbers, highly crystalline MAH-g-EPDM rubber, containing 30% crystalline PP (EPDM-C) and amorphous MAH-g-EPDM rubber (EPDM-A), were used as a mixture for adhesion between Al foil and CPP. This was done because EPDM-C can largely improve mechanical properties as well as expand the film's applications while EPDM-A can impart easy film formation [25–29]. To facilitate not only homogenous mixing between EPDM-C and EPDM-A but also efficient penetration of adhesives into the CPP surface, EPDM-C and EPDM-A were mixed with 15 wt.% of highly reactive polybutene (HRPB), which has a low molecular weight (M_W) and is highly compatible with CPP. Furthermore, the double bonds (C=C) of HRPB result in the high cross-linking with CPP and the MAH-g-EPDM rubbers during curing and tempering process with azobisbutylnitrile (AIBN), a radical initiator. The HRPB played important role as not only an excellent compatibilizer for MAH-g-EPDM rubbers but also a latent crosslinker for the adhesives and CPP, resulting in a great improvement in the peel strength of CPP/Al foil laminates.

The relatively weak adhesion between Al foil and MAH-g-EPDM rubbers resulting from their different polarities can cause the adhesive to fail on the Al foil. In this study, the poor adhesion between Al foil and MAH-g-EPDM rubbers was ameliorated by coating the surface of Al foil with (3-aminopropyl)triethoxysilane (APTES) via silanization. The free –NH groups of APTES reacted with the MAH groups of MAH-g-EPDM rubbers to form imide bonds. Introducing strong imide bond at the interface between Al foil and MAH-g-EPDM rubbers accompanied the largely enhanced the peel strength of CPP/Al foil laminates causing the cohesive failures in 180° peel test. In this study, we investigated new types of adhesives prepared from two types of MAH-g-EPDM rubbers and HRPB that generate strong adhesion between CPP film and Al foil. The prepared adhesive showed good compatibility with CPP and the introduction of imide bonds at the interface between MAH-g-EPDM rubbers and Al foil greatly improved the peel strength of CPP/Al foil laminates. We also studied the effects of the composition of adhesives, adhesive thickness and tempering on the peel strength of CPP/Al foil laminates for practical applications.

2. Experiment

2.1. Materials

CPP films (thickness: 40 μm) and Al foil (thickness: 80 μm) foils were supplied from LG Chem in Dae-jeon, Korea. Two kinds of MAH-g-EPDM rubbers, EPDM-A (KEPA-1150) and EPDM-C (KEPA-1130), were purchased from Kumho Polychem in Dae-jeon, Korea. EPDM-A is amorphous while EPDM-C is semi-crystalline due to the presence of 30 wt.% PP. According to the supplier, both EPDM-A and EPDM-C are based on MAH-g-terpolymers of ethylene, propylene and ethylidene norbornene (ENB) in which MAH contents are 0.7 wt.%. HRPB (HRPB 750, M_W: 770 g/mol) was obtained from Daelim Industry in Yeo-su, Korea. APTES and acetic acid, which were used to modify the surface of Al foil, were purchased from Sigma-Aldrich Chemical in Yong-in, Korea. Xylene was used as solvent for the mixtures of EPDM-A, EPDM-C and HRPB. AIBN was used as a radical initiator for cross-linking the adhesives and CPP. Both xylene and AIBN were also purchased from Sigma-Aldrich Chemical in Korea. All chemicals were used as received. The chemical structures of the raw materials are presented in Figure 1.

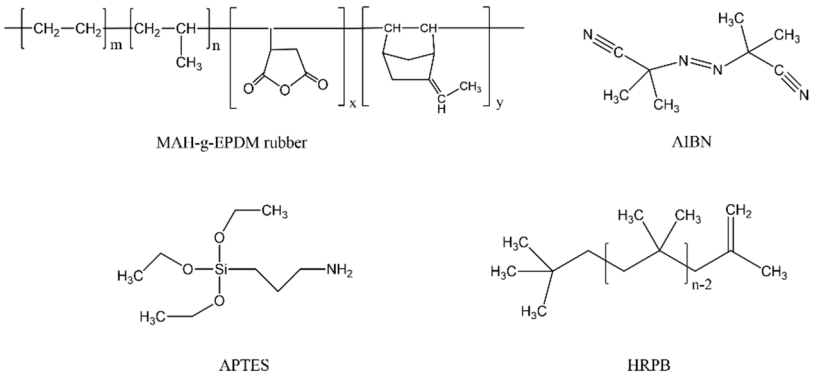

Figure 1. Chemical structures of the raw materials.

2.2. Adhesive Preparation

All adhesive samples were prepared by solvent mixing. Xylene was used as solvent to dissolve EPDM-A/EPDM-C to produce a homogeneous mixture. The EPDM-A/EPDM-C mixture (70/30 by wt.%) was placed in a four-necked flask under nitrogen purging. HRPB (0–25 wt.% of MAH-g-EPDM rubbers) was then added to the flask followed by adding xylene to prepare a solution of fixed solid content (10% by wt). Subsequently, the solution was mechanically stirred at 110 °C for 1 h to obtain a homogeneous mixture of EPDM-A/EPDM-C and HRPB.

2.3. Modification of Al Surface

To introduce strong chemical bonds between Al foil and the adhesive, the surface of Al foil was chemically treated with APTES. A 1 wt.% solution of APTES in water was prepared at room temperature. Subsequently, the pH of the solution was adjusted to 5 by adding acetic acid dropwise under stirring. The prepared APTES solution was homogeneously spray-coated on the surface of Al foil. The APTES-coated Al foil samples were placed in a convection oven at 110 °C for 1 h to modify surface of Al foil, facilitating the formation of strong chemical bonds between APTES and Al foil via silanization. The treatments were based on the sol-gel reactions of silane coupling agent on the Al as reported in the literature [47].

2.4. Adhesive Coating on Al Foil and Lamination with CPP

The prepared EPDM-rubber-based adhesive dissolved in xylene were mechanically mixed with 1, 3 or 5 wt.% of AIBN at room temperature to obtain homogeneous mixtures, which were then coated on APTES-coated Al foil. Uniform adhesive thickness was obtained using a bar coater and the thickness of adhesive layer was measured with a micrometer. To remove solvent, samples were placed in a vacuum oven at 80 °C for 120 s. Finally, CPP was placed on the dried adhesive-coated Al foil and laminated at 110 °C with a speed of 10 mm/s for the efficient penetration of the adhesive from the Al foil up to the CPP film. To evaluate the effect of tempering, the samples were aged in a convection oven at 80 °C for 5 days.

In this study, adhesion between Al foil and CPP film was facilitated by using mixture of two types of MAH-g-EPDM rubbers and HRPB as an adhesive. To improve the weak adhesion between the adhesive and the Al foil, the surface of the Al foil was treated with APTES, resulting in the formation of strong imide bonds between APTES and MAH-g-EPDM rubbers during the lamination step. The imide bonds caused strong adhesion between CPP and APTES-treated-Al foil. Tempering at 80 °C further enhanced the interfacial interaction between the adhesive and the CPP via the radical polymerization of MAH-g-EPDM rubbers and HRPB, which was used to not only increase the compatibility between the different kinds of MAH-g-EPDMs but also facilitate the easy penetration of the adhesive based on its good compatibility with CPP. The overall process is illustrated in Figure 2.

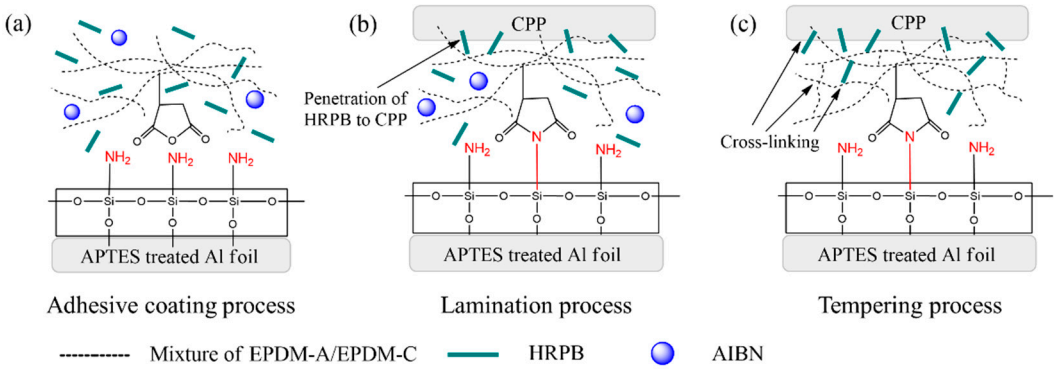

Figure 2. Overall scheme for CPP and Al foil adhesion. (**a**) The prepared adhesive is uniformly coated on the APTES treated Al foil using a bar coater; (**b**) The EPDM-A/EPDM-C form maleimide groups via imidization with the $-NH_2$ groups of APTES and wet onto CPP during lamination at 110 °C; (**c**) The mixture of EPDM-A/EPDM-C and HRPB form a cross-linked structure with CPP via radical polymerization during tempering.

2.5. Characterization

The 180° peel test was conducted for all prepared laminated samples on a universal testing machine (UTM) (LR5K Plus, LLOYD, West Sussex, UK). The width and length of samples were fixed at 15 and 60 mm, respectively and the tests were conducted at room temperature with a crosshead speed of 250 mm/min. The peel strength was determined by using following equation,

$$\text{Peel strength} = F/w \quad (1)$$

where F is the average peel force (N) and w is the width of specimen (mm). The peel tests of CPP/adhesive/Al foil laminates were conducted with 5 specimens per sample and the average values were taken for the analyses. The thermal properties of the prepared EPDM based adhesive and raw material were evaluated by differential scanning calorimetry (DSC) (TA, Q20, New Castle, DE, USA). DSC was calibrated using around 5 mg of indium as a standard for the quantitative measurements. The DSC measurement was performed from −80 to 200 °C in N_2 gas environment at a heating rate of 10 °C/min twice for the samples. The APTES coating and imidization between APTES and

the MAH of the adhesive were analyzed by energy-dispersive X-ray analysis (EDX) (SUPRA 40VP, Carl Zeiss, Oberkochen, Germany) and Fourier transform infrared spectroscopy (FT-IR) (FT/IR 300E, JASCO, Easton, MD, USA). The FT-IR spectra were collected in ATR mode using a diamond crystal at 4 cm^{-1} resolution from 4000 to 500 cm^{-1} by scanning 100 times for the samples. The field-emission scanning electron microscope (FE-SEM) (SUPRA 40VP, Carl Zeiss, Germany) was used to analyze the morphologies of the adhesion surfaces after peel testing. For the measurement via EDX and FE-SEM, the surfaces of peel tested samples were coated with conductive gold (Au) layer.

3. Results and Discussion

3.1. Adhesion Based on EPDM-A, EPDM-C and HRPB

Many parameters can affect the adhesion strengths of adhesives. In this study, we evaluated the effects of adhesive composition, concentration of radical initiator, adhesive thickness and thermal tempering. Two kinds of MAH-g-EPDM rubbers, EPDM-A and EPDM-C, were tested as the adhesives between CPP and Al foil. EPDM-A is amorphous and shows good affinity for CPP during coating. In contrast, EPDM-C contains 30 wt.% PP. Although the crystallinity of EPDM-C may result in better mechanical properties, it cannot exclusively be used as the adhesive because its crystallinity results in limited film formation on Al foil on drying. Thus, mixture of EPDM-C and EPDM-A in xylene was prepared and HRPB was subsequently added to improve the compatibility between EPDM-C and EPDM-A. The mixtures were initially tested with various weight compositions. For example, when the content of EPMD-C exceeded 30 wt.%, the mixture lost flowability. Thus, the mixing ratio of EPMD-A:EPDM-C was fixed at 7:3 by weight to obtain MAH-g-EPDM rubber blends (EMPD-B).

Figure 3 shows the peel strengths of CPP/Al foil laminates without tempering, which were laminated by EPDM-B or EPDM-A with different HRPB contents. The thickness of adhesives was fixed at 15 μm and it was well-controlled by employing a bar coater during adhesive application on Al foil. Compared with EPDM-A-based CPP/Al laminates, EPDM-B-based CPP/Al laminates showed much higher peel strengths regardless of the HRPB content because 30 wt.% of crystalline PP in EPDM-C might introduce large enhancement in the modulus and yield strength of adhesive itself [25,26,48,49]. The peel strength of CPP/Al foil laminate increased with increasing HRPB content until 15 wt.%, after which the peel strength decreased. These results indicate that the optimal adhesive for CPP/Al laminate is the EPDM-B, containing 15 wt.% of HRPB (EPDM-B-15).

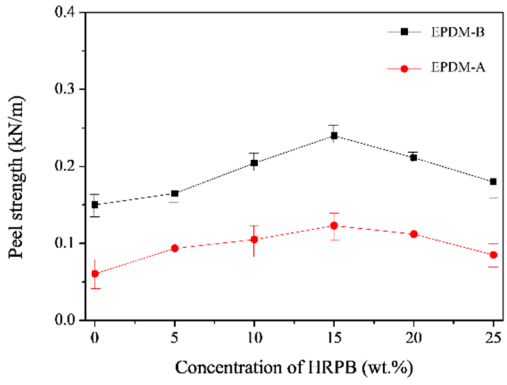

Figure 3. Peel strengths of CPP/Al foil laminates vs HRPB (wt.%) content of the adhesives, which were laminated with EPDM-B (■) or EPDM-A (●). The failures occurred at interfaces of adhesives and Al foils regardless of concentration of HRPB.

Figure 4a shows the DSC traces of the raw materials, EPDM-B and EPDM-B-15; the results are summarized in Table 1. The melting point (T_m) of EPDM-C was approximately 168 °C, which is attributed to the crystallinity of PP. In contrast, the T_m of EPDM-A was not observed because of its amorphous nature. EPDM-B, the mixture of EPDM-C and EPDM-A, showed a slight decrease of T_m

compared with EPDM-C. It was expected the enthalpy change (ΔH_m) at T_m of EPDM-B would be about 7 J/g based on the EPDM-C content (30 wt.%) of the EPDM-B. It is of interest to note the ΔH_m of EPDM-B was 16 J/g possibly due to the nucleation effect of crystalline PP in the system. On the other hand, when EPDM-B compatibilized with 15 wt.% of HRPB, the T_m of EPDM-B decreased from 167 to 162 °C and the peak intensity also greatly reduced because of a decrease in the crystallinity of EPDM-C. Specifically, the ΔH_m of EPDM-C also decreased from 24 to 5 J/g in the presence of HRPB. The large decrease in T_m and ΔH_m implies that HRPB was an effective compatibilizer and caused the crystallinity of EPDM-C to decrease upon mixing with EPDM-A.

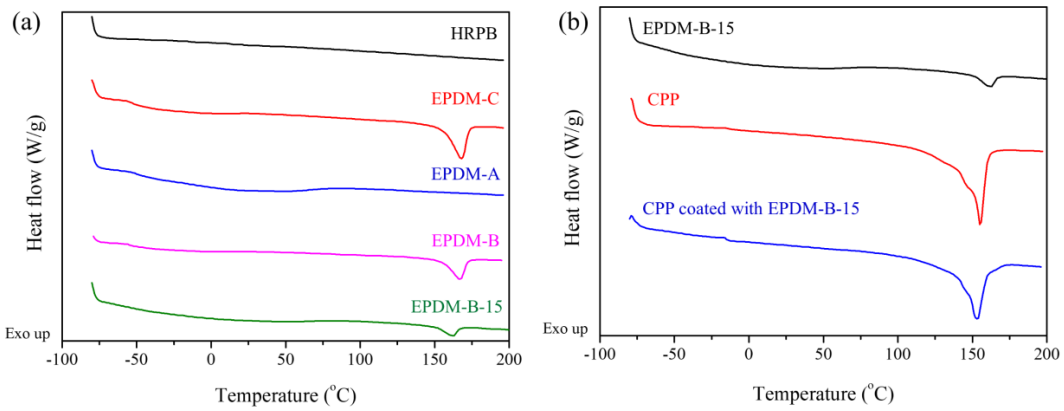

Figure 4. DSC thermograms during heating for (**a**) raw materials and EPDM-B-15 and (**b**) EPDM-B-15, CPP film and CPP coated with EPDM-B-15.

Table 1. Results of DSC thermogram.

Thermal Properties	Samples				
	EPDM-C	EPDM-B	EPDM-B-15	CPP	CPP Coated with EPDM-B-15
T_m (°C)	168	167	162	155	152
ΔH_m (J/g)	24	16	5	50	38

The DSC thermograms also confirmed the excellent affinity between CPP and EPDM-B-15. Figure 4b shows the DSC curves of EPDM-B-15, CPP and CPP coated with 5-μm-thick EPDM-B-15 at 110 °C. The solvent in EPDM-B-15 and CPP coated with EPDM-B-15 was fully removed in convection oven at 80 °C for 1 day. Although only 5 μm of EPDM-B-15 was coated on CPP (The weight ratio of coated EPDM-B-15 and CPP was 1:8.5), EPDM-B-15 caused the T_m of CPP to decrease from 155 to 152 °C and the ΔH_m of CPP to decrease from 50 and 38 J/g. Considering that EPDM-B-15 has a higher T_m than CPP (T_m of EPDM-B-15 and CPP: 162 and 155 °C respectively), the significant decrease in T_m of CPP after coating with EPDM-B-15 is a result of the high crystallinity of CPP, lowered by HRPB in EPDM-B-15. The possible penetration of HRPB to CPP was confirmed by the swelling of CPP in HRPB as described in Table S1 of Supplementary material. These results indicate that EPDM-B-15 showed good compatibility with CPP and the crystallinity of CPP was suppressed by the penetration of HRPB in EPDM-B-15.

We also evaluated the effect of the concentration of radical initiator (AIBN) on peel strength of CPP/Al foil laminate (Figure 5). The addition of AIBN was expected to introduce cross-linking among the EPDM-B-15 and CPP via free-radical polymerization. EPDM-B-15 adhesives containing different amounts of AIBN (0, 1, 3 and 5 wt.%) were prepared and evaluated for the CPP/Al laminates. The EPDM-B-15/AIBN mixture was coated on the Al substrate with a thickness of 10 μm and laminated at 110 °C with CPP. After 1 day of tempering at 80 °C, laminates of CPP/Al foil were evaluated by peel testing. The addition of AIBN generally increased the peel strength of CPP/EPDM-B-15/Al foil laminates, although the peel strength was maximized at the AIBN content of 1 wt.% (Figure 5).

The decrease in peel strength upon the addition of larger amounts of AIBN may have resulted from the chain scission of EPDM-B-15 main chains; it was previously reported that excess active free radicals might have caused the main-chain scission of the MAH-g-EPDM or PP in MAH-g-EPDM, resulting in a decrease in the MW of the main backbones or disproportionation during cross-linking process [50–52]. On the basis of these results, an in EPDM-B-15 containing 1 wt.% of AIBN content was used in subsequent experiments. Although the incorporation of AIBN resulted in a significant increase in the peel strength of the laminates, adhesive failure was observed at the interface between the adhesive and Al foil as shown in Figure S1 in Supplementary material. In order to improve the adhesion between the adhesive and Al foil, Al foil was treated with silane coupling agent, 3-aminopropyl triethoxysilane (APTES), to induce cohesive failure via chemical bonding of Al foil with MAH of EPDM.

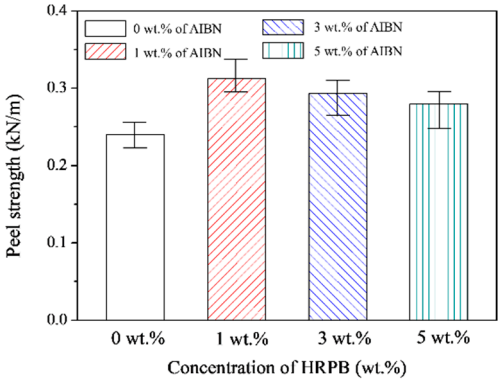

Figure 5. Effect of radical initiator content on the peel strength of EPDM-B-15-based CPP/Al foil laminates. The failure occurred at interfaces between EPDM-B-15 and Al foil regardless of concentration of AIBN.

3.2. Surface Treatment of Al Foil with APTES

To introduce strong chemical bonds and obtain strong adhesion between EPDM-B-15 and Al foil, the Al surface was coated with APTES and thermally treated at 100 °C following the process reported by Denoyelle et al. and Plueddemann [47,52]. The processes are described in Section 2.3 and schematically presented in Figure 6.

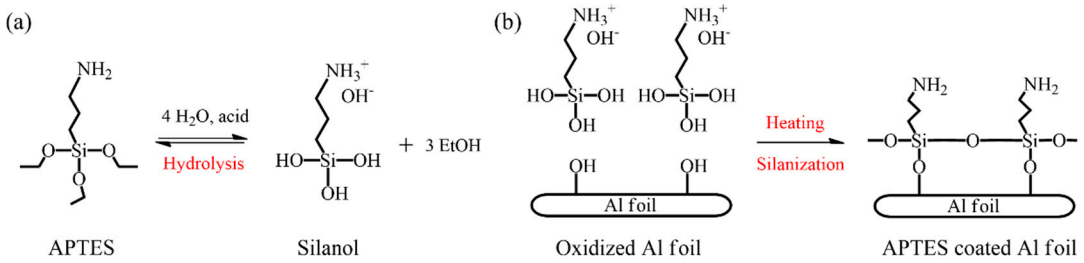

Figure 6. Mechanism for the surface treatment of Al foil with APTES: (**a**) hydrolysis of APTES in acidic condition; (**b**) silanization between oxidized Al foil and silanol.

Figure 7a,b show the SEM and EDX results of the Al foil and APTES treated Al foil after peel test. As shown in the SEM images, no visible differences in surface morphology were observed between Al foil and APTES-treated Al foil because of the thin layer of APTES coated on the Al foil. However, the EDX data show obvious differences in surface composition between Al foil and APTES-treated Al. Only two elements, Al and oxygen (O), were detected in Al foil. The small amount of O detected in Al foil implies that Al was easily oxidized without thermal or chemical treatment in the air. In contrast, carbon (C), O and silicon (Si) were detected on the APTES-treated Al foil surface and oxygen content also largely increased, indicating the successful treatment with APTES. The APTES

treatment was also confirmed by FT-IR (Figure 7c). No visible peaks are seen in the spectrum of Al foil. In contrast, the spectrum of APTES-treated Al foil shows peaks corresponding to –CH stretching (symmetric and asymmetric) at 2900 and 2860 cm^{-1} along with –NH peaks at 3300 and 3370 cm^{-1}. These peaks are the characteristic of the hydrocarbon chains and primary amine groups of APTES. In addition, Si–O stretching peaks were detected at 1200 cm^{-1}. The –Si–O peak at 1000 cm^{-1} is attributed to the formation of an Si–O–Si network resulting from the silanization of APTES. The peaks at 3500 cm^{-1} (–OH of silanol) and 920 cm^{-1} (Si–O–Et of APTES) provide some evidence for the incomplete hydrolysis and silanization of APTES; however, the formation of Si–O–Si networks on the Al surface, as demonstrated by the FT-IR spectra, suggest that most of APTES participated in the treatment [53].

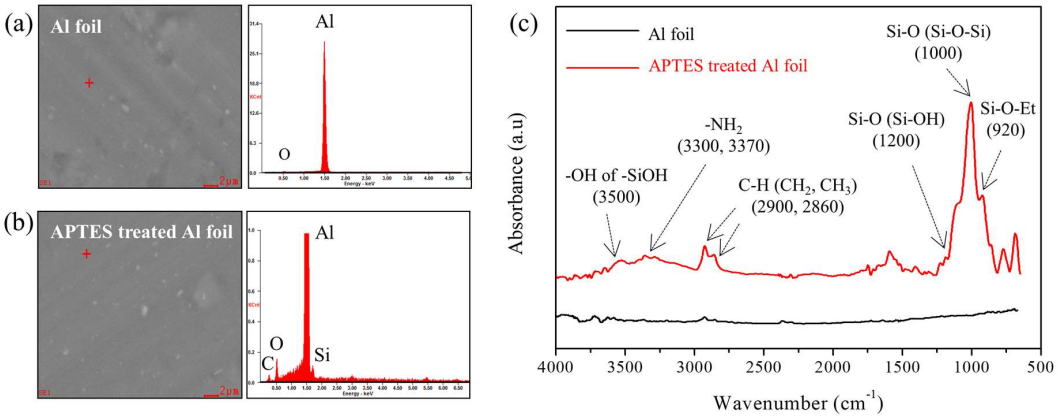

Figure 7. SEM images and EDX data of Al foil (**a**), APTES-treated Al foil (**b**) and FT-IR spectra of Al foil and APTES-treated Al foil (**c**).

The highly reactive –NH_2 group of APTES, which persists even after the treatment process on Al foil, provide chemically active sites for reaction with the MAH groups of MAH-g-EPDM rubbers. Many researchers have reported that strong imide bonds can be formed via ring-opening and cyclization reactions between amine and MAH groups [40–46,54,55]. Nuclear magnetic resonance and FT-IR analysis could be the most powerful tools for confirming the formation of imide bonds between APTES-treated Al foil and EPDM-B-15; however, these methods could not be employed in this study because of the low proportion of imide bonds within the CPP/EPDM-B-15/APTES-treated Al foil laminates. Thus, we directly reacted EPDM-A with APTES in the presence of solvent to verify the feasibility of imidization under lamination temperatures of 110 °C.

Figure 8 shows the scheme of imidization between the MAH groups of EPDM-A and –NH_2 groups of APTES. Imidization of APTES and EPDM-A was conducted and 110 °C for 15 min with magnetic stirring in xylene and monitored by FT-IR. To confirm the formation of imide linkage, we monitored the peaks at 1860 cm^{-1}, which correspond to the asymmetric stretching of anhydride carbonyl groups (C=O) of MAH in EPDM-A; after the imidization with APTES, these peaks were disappeared, providing strong evidence of reaction of MAH groups of EPDM-A for imidization at 110 °C in the laminator. The characteristic anhydride symmetric carbonyl stretching at 1786 cm^{-1} and carboxylic groups stretching at 1711 cm^{-1} were also monitored. The peak at 1786 cm^{-1} was shifted to low wavenumbers (1779 cm^{-1}) with strong decrease in intensity. On the other hand, the peak at 1711 cm^{-1} shows the significant increase in its intensity with shifting to 1707 cm^{-1} due to the formation of imide groups [55,56]. These results imply that imide bonds were formed between the EPDM-A and APTES-treated Al foil after lamination at 110 °C. These imide bonds are expected to greatly improve the peel strength of CPP/Al foil laminates by preventing adhesion failure between adhesives and Al foil.

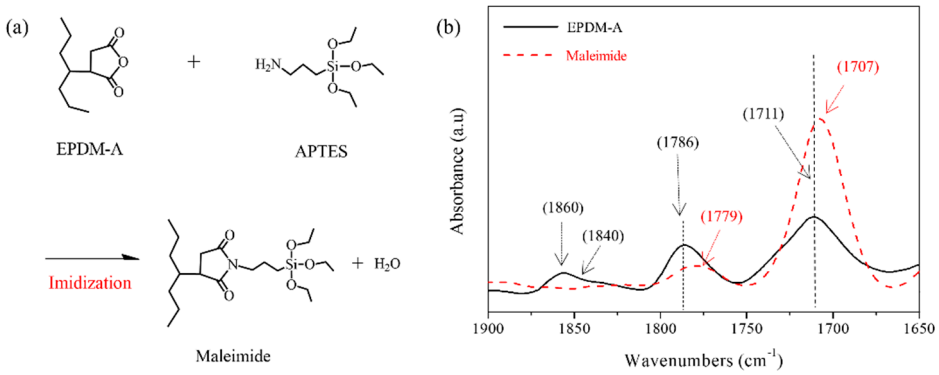

Figure 8. Schematic for the imidization of the MAH groups of EPDM-A and amine groups of APTES (**a**) and FT-IR spectra of EPDM-A (black) and maleimide synthesized from reaction between EPDM-A and APTES (red dot line) (**b**).

3.3. Adhesive Strength of CPP/APTES-Treated Al Foil Laminates

Silane treatment on the Al surface with APTES was expected to largely improve the weak adhesion between Al foil and EPDM-B-15 through imidization (see Figure 8). Improved adhesion between APTES-treated Al foil and EPDM-B-15 was confirmed via the 180° peel strength. The results of peel testing are shown in Figure 9a,b. Figure 9a depicts the peel force versus extension curve and Figure 9b depicts peel strength of CPP/EPDM-B-15/Al foil and CPP/EPDM-B-15/APTES-treated Al foil after tempering at 80 °C for 1day. As shown in Figure 9, CPP/EPDM-B-15/APTES-treated Al foil shows a much higher average peel force (7.85 N) and peel strength (0.54 kN/m) than those of CPP/EPDM-B-15/Al foil (average peel force: 4.68 N, peel strength: 0.31 kN/m). The significant improvement in peel force and peel strength of CPP/EPDM-B-15/APTES-treated Al foil, around 42%, can be attributed to the enhanced adhesion between APTES-treated Al foil and EPDM-B-15 by the formation of maleimide bond.

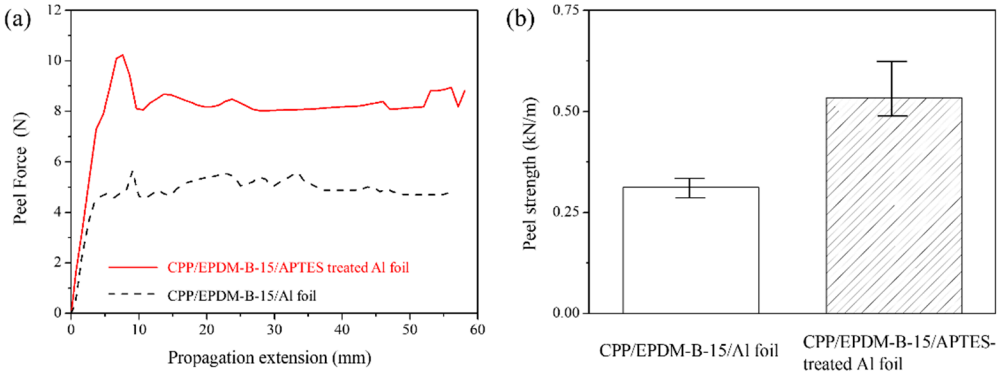

Figure 9. Results of the 180° peel test after tempering at 80 °C for 1 day: (**a**) typical peel force (N) vs. propagation extension (mm) of CPP/EPDM-B-15/APTES-treated Al foil and CPP/EPDM-B-15/Al foil, (**b**) peel strength (kN/m) of CPP/EPDM-B-15/APTES-treated Al foil and CPP/EPDM-B-15/Al foil.

When Al foil and CPP were laminated with EPDM-B-15 and subjected to peel testing after 1 day of tempering, adhesive failure on the Al surface occurred. As shown if Figure 10a, after peel testing, the smooth and bare surface of Al foil was observed due to the adhesive failure between Al foil and EPDM-B-15. This indicates that the adhesion between Al foil and EPDM-B-15 without chemical bonding is much weaker compared with that between CPP and EPDM-B-15 crosslinked by radical polymerization. In contrast, cohesive failure of the adhesives occurred in CPP/EPDM-B-15/APTES-treated Al foil, which was observed on the surface of APTES-treated Al foil, as shown in Figure 10b. Moreover, the EDX results on the assigned area in SEM images

presented that the CPP/EPDM-B-15/APTES-treated Al foil showed a much higher amount of C element than CPP/EPDM-B-15/Al foil and almost no Al element was found due to the full coverage of Al foil surface with EPDM-B-15. This is further strong evidence that the introduction of imine bond enhances the adhesion between the adhesive and the Al foil. It is speculated that the cohesive failure of EPDM-B-15 was caused by strong adhesion at the both interfaces of EPDM-B-15/CPP and EPDM-B-15/APTES-treated Al foil resulting from the cross linking and strong imide chemical bonds respectively.

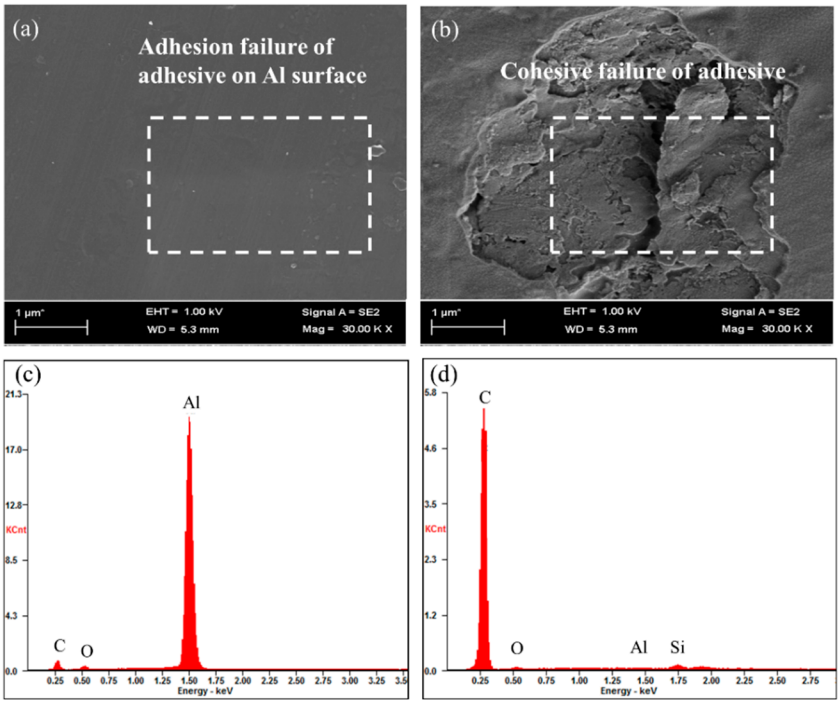

Figure 10. SEM images and EDX results of the Al surfaces of CPP/EPDM-B-15/Al foil and CPP/EPDM-B-15/APTES-treated Al foil laminates after peel test. The peel test was conducted after tempering of the laminates at 80 °C for 1 day: (**a**) Al surface of CPP/EPDM-B-15/Al foil; (**b**) APTES-treated Al foil surface of CPP/EPDM-B-15/APTES-treated Al foil; (**c**,**d**) EDX results in the area assigned with white dotted line in (**a**) and (**b**) respectively.

Figure 11 shows the adhesion of CPP/EPDM-B-15/Al foil and CPP/EPDM-B-15/APTES-treated Al foil laminated with different thickness of EPDM-B-15 and aged for various times at 80°C. The peel strength increased with increasing adhesive thickness in the tempering time range that was investigated, regardless of the presence of APTES on Al. The peel strength of CPP/EPDM-B-15/APTES-treated Al foil significantly increased with an increasing thickness of EPDM-B-15 with cohesive failure of EPDM-B-15 (Figure 10b). However, when compared with CPP/EPDM-B-15/APTES-treated Al foil, the CPP/EPDM-B-15/Al foil was found to show relatively little improvement in peel strength with time for tempering. Furthermore, the significant improvement in peel strength was not observed above 45 µm. This trend was mainly attributed to the weak interfacial adhesion between EPDM-B-15 and Al foil substrate that resulted in an adhesive failure on the Al surface during the peel test (Figure 10a). These findings strongly suggest that a significant increase in peel strength depending on the thickness is possible with strong adhesion of EPDM-B-15, with both APTES-treated Al foil and CPP exhibiting cohesive failure. Thermal tempering time also affected the peel strength. Radical polymerization largely depends on the half-life time of the radical initiator: the half-life of the initiator used in this study (AIBN) was 80 min at 80 °C [57]. Although the theoretical time for the consumption of AIBN in radical polymerization is approximately 14 h, tempering times of up to 5 days were studied to provide sufficient free-radical-induced crosslinking

time. Adhesive strength gradually increased with increasing tempering time up to 3 days in both CPP/EPDM-B-15/APTES-treated Al foil and CPP/EPDM-B-15/Al foil laminates. This indicates that tempering times longer than the half-life of the radical initiator is effective for implementing high cross-linking between CPP and EPDM-B-15, which results in a significant improvement in peel strength.

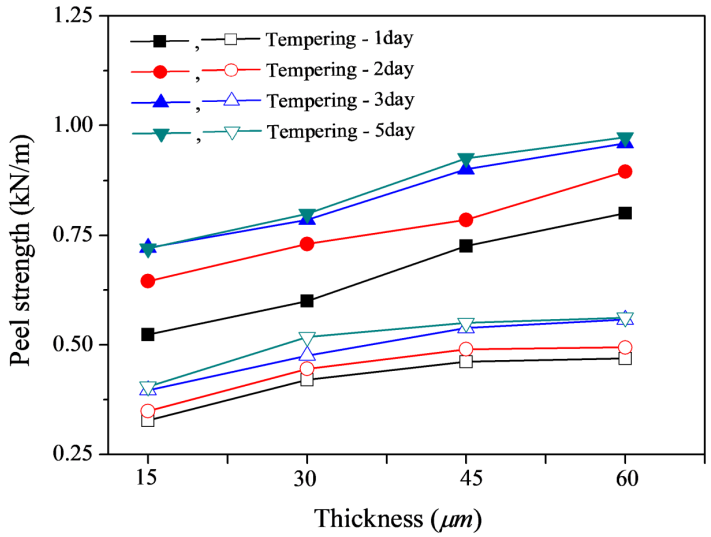

Figure 11. Effects of adhesive thickness and tempering time on the adhesive strength of CPP/EPDM-B-15/Al foil (open symbol) and CPP/EPDM-B-15/APTES-treated Al foil (filled symbol).

4. Conclusions

The peel strength between Al foil and CPP film could be enhanced by using MAH-g-EPDM-rubber-based adhesives for the lamination. The addition of HRPB to the adhesive not only enhanced the compatibility between the two kinds of MAH-g-EPDM rubbers having different crystallinities but also helped the adhesive penetrate and cross-link with CPP. In addition, the relatively weak interfacial adhesion between the EPDM-B-15 and Al foil, which resulted in adhesive failure on the Al surface, was enhanced by introducing imide bonds via the treatment of the Al foil with APTES. The formation of imide bonds between the MAH groups of the adhesive and the –NH groups of APTES, which was coated on Al foil, resulted in the cohesive failure of the adhesive during peel testing. The effects of the composition of adhesives, tempering time and adhesive thickness on peel strength of CPP/Al foil laminates were also studied to optimize the adhesion. We infer that MAH-g-EPDM-based adhesives can be applied in various laminations of polyolefin films and Al foils for packaging of foods, electronic devices and lithium-ion batteries.

Supplementary Materials: The following are available online at http://www.mdpi.com/2079-6412/9/1/61/s1, Table S1: Results of swelling test of CPP in HRPB at 80 °C for 1 day, Figure S1: (a,b) SEM image and FT-IR spectra of CPP side after peel testing of CPP/EPDM-B-15/Al foil; (c,d) SEM image and FT-IR spectra of Al foil side after peel testing of CPP/EPDM-B-15/Al foil.

Author Contributions: Conceptualization, D.-S.L. and S.-W.Y.; Methodology, E.-S.P. and J.-Y.H.; Investigation, E.-S.P., J.-Y.H., S.-H.L. and D.-S.L.; Writing–Original Draft Preparation, S.-H.L.; Writing–Review & Editing, D.-S.L.; Project Administration, D.-S.L. and S.-W.Y.

Funding: This research was funded by LG Chem.

Conflicts of Interest: The authors declare no conflict of interest.

References

1. Xia, F.; Xu, S. Effect of surface pre-treatment on the hydrophilicity and adhesive properties of multilayered laminate used for lithium battery packaging. *Appl. Surf. Sci.* **2013**, *268*, 337–342. [CrossRef]
2. Nakai, M.; Eto, T. New aspects of development of high strength aluminum alloys for aerospace applications. *Mater. Sci. Eng. A* **2000**, *285*, 62–68. [CrossRef]
3. Subasri, R.; Jyothirmayi, A.; Reddy, D.S. Effect of plasma surface treatment and heat treatment ambience on mechanical and corrosion protection properties of hybrid sol-gel coatings on aluminum. *Surf. Coat. Technol.* **2010**, *205*, 806–813. [CrossRef]
4. Joshi, S.P.; Toma, R.B.; Medora, N.; O'Connor, K. Detection of aluminium residue in sauces packaged in aluminium pouches. *Food Chem.* **2003**, *83*, 383–386. [CrossRef]
5. Keles, O.; Dundar, M. Aluminum foil: Its typical quality problems and their causes. *J. Mater. Process. Technol.* **2007**, *186*, 125–137. [CrossRef]
6. Byun, Y.; Bae, H.J.; Cooksey, K.; Whiteside, S. Comparison of the quality and storage stability of salmon packaged in various retort pouches. *LWT Food Sci. Technol.* **2010**, *43*, 551–555. [CrossRef]
7. Ashley, R.J.; Cochran, M.A.; Allen, K.W. Adhesives in packaging. *Int. J. Adhes. Adhes.* **1995**, *15*, 101–108. [CrossRef]
8. Zand, B.N.; Mahdavian, M. Corrosion and adhesion study of polyurethane coating on silane pretreated aluminum. *Surf. Coat. Technol.* **2009**, *203*, 1677–1681. [CrossRef]
9. Zand, B.N.; Mahdavian, M. Evaluation of the effect of vinyltrimethoxysilane on corrosion resistance and adhesion strength of epoxy coated AA1050. *Electrochim. Acta* **2007**, *52*, 6438–6442. [CrossRef]
10. Niknahad, M.; Moradian, S.; Mirabedini, S.M. The adhesion properties and corrosion performance of differently pretreated epoxy coatings on an aluminium alloy. *Corros. Sci.* **2010**, *52*, 1948–1957. [CrossRef]
11. Leena, K.; Athira, K.K.; Bhuvaneswari, S.; Suraj, S.; Rao, V.L. Effect of surface pre-treatment on surface characteristics and adhesive bond strength of aluminium alloy. *Int. J. Adhes. Adhes.* **2016**, *70*, 265–270. [CrossRef]
12. Xu, Y.; Li, H.; Shen, Y.; Liu, S.; Wang, W.; Tao, J. Improvement of adhesion performance between aluminum alloy sheet and epoxy based on anodizing technique. *Int. J. Adhes. Adhes.* **2016**, *70*, 74–80. [CrossRef]
13. Chen, H.; Wang, J.; Huo, Q. Self-assembled monolayer of 3-aminopropyltrimethoxysilane for improved adhesion between aluminum alloy substrate and polyurethane coating. *Thin Solid Films* **2007**, *515*, 7181–7189. [CrossRef]
14. Taniguchi, T. Packaging Material for Lithium Ion Battery. U.S. Patent 9,601,724, 21 March 2017.
15. Taniguchi, T. Outer Package Material for Lithium-on Battery and Method for Producing Lithium-on Battery Using the Outer Package Materal. U.S. Patent 9,627,660, 18 April 2017.
16. Liang, C.; Lv, Z.; Bo, Y.; Cui, J.; Xu, S. Effect of modified polypropylene on the interfacial bonding of polymer—Aluminum laminated films. *J. Mater.* **2015**, *81*, 141–148. [CrossRef]
17. Shin, K.S.; Kim, K.J.; Choi, S.-W.; Rhee, M.H. Mechanical properties of aluminum/polypropylene/aluminum sandwich sheets. *Met. Mater.* **1999**, *5*, 613–618. [CrossRef]
18. Nielsen, A.S.; Batchelder, D.N.; Pyrz, R. Estimation of crystallinity of isotactic polypropylene using raman spectroscopy. *Polymer* **2002**, *43*, 2671–2676. [CrossRef]
19. Parenteau, T.; Ausias, G.; Grohens, Y.; Pilvin, P. Structure, mechanical properties and modelling of polypropylene for different degrees of crystallinity. *Polymer* **2012**, *53*, 5873–5884. [CrossRef]
20. Tall, S.; Albertsson, A.C.; Karlsson, S. Enhanced rigidity of recycled polypropylen from packaging waste by compounding with talc and high crystallinity polypropylene. *Polym. Adv. Technol.* **2001**, *12*, 279–284. [CrossRef]
21. Wang, K.H.; Choi, M.H.; Koo, C.M.; Choi, Y.S.; Chung, I.J. Synthesis and characterization of maleated polyethylene/clays nanocomposites. *Polymer* **2001**, *42*, 9819–9826. [CrossRef]
22. Baldwin, F.P.; Strate, G.V. Polyolefin elastomers based on ethylene and propylene. *Rubber Chem. Technol.* **1972**, *45*, 709–881. [CrossRef]
23. Cesca, S. The chemistry of unsaturated ethylene-propylene based terpolymers. *J. Polym. Sci. Macromol. Rev.* **1975**, *10*, 1–230. [CrossRef]

24. Grestenberger, G.; Potter, G.D.; Grein, C. Polypropylene/ethylene-propylene rubber (PP/EPR) blends for the automotive industry: Basic correlations between EPR-design and shrinkage. *Express Polym. Lett.* **2014**, *8*, 282–292. [CrossRef]
25. Danesi, S.; Porter, R.S. Blends of isotactic polypropylene and ethylene-propylene rubbers: Rheology, morphology and mechanics. *Polymer* **1978**, *19*, 448–457. [CrossRef]
26. Greco, R.; Mancarella, C.; Martuscelli, E.; Ragosta, G.; Yin, J. Polyolefin blends: 2. Effect of EPR composition on structure, morphology and mechanical properties of IPP/EPR alloys. *Polymer* **1987**, *28*, 1929–1936. [CrossRef]
27. Karger-Kocsis, J.; Kalló, A.; Kuleznev, V.N. Phase structure of impact-modified polypropylene blends. *Polymer* **1984**, *25*, 279–286. [CrossRef]
28. Pukanszky, B.; Tüdös, F.; Kallo, A.; Bodor, G. Effect of multiple morphology on the properties of polypropylene/ethylene-propylene-diene terpolymer blends. *Polymer* **1987**, *30*, 1407–1413. [CrossRef]
29. Van Der Wal, A.; Gaymans, R.J. Polypropylene-rubber blends: 5. Deformation mechanism during fracture. *Polymer* **1999**, *40*, 6067–6075. [CrossRef]
30. Gaca, M.; Zaborski, M. The Properties of ethylene–propylene elastomers obtained with the use of a new cross-linking substance. *J. Therm. Anal. Calorim.* **2016**, *125*, 1105–1113. [CrossRef]
31. Polgar, L.M.; Kingma, A.; Roelfs, M.; van Essen, M.; van Duin, M.; Picchioni, F. Kinetics of cross-linking and de-cross-linking of EPM rubber with thermoreversible Diels-Alder chemistry. *Eur. Polym. J.* **2017**, *90*, 150–161. [CrossRef]
32. Zhang, H.; Datta, R.N.; Talma, A.G.; Noordermeer, J.W.M. Maleic-anhydride grafted EPM as compatibilising agent in NR/BR/EPDM blends. *Eur. Polym. J.* **2010**, *46*, 754–766. [CrossRef]
33. Grigoryeva, O.P.; Karger-Kocsis, J. Melt grafting of maleic anhydride onto an ethylene-propylene-diene terpolymer (EPDM). *Eur. Polym. J.* **2000**, *36*, 1419–1429. [CrossRef]
34. Manjhi, S.; Sarkhel, G. Effect of maleic anhydride grafted ethylene propylene diene monomer (MAH-g-EPDM) on the properties of kaolin reinforced EPDM rubber. *J. Appl. Polym. Sci.* **2011**, *119*, 2268–2274. [CrossRef]
35. Pasbakhsh, P.; Ismail, H.; Fauzi, M.N.A.; Bakar, A.A. Influence of maleic anhydride grafted ethylene propylene diene monomer (MAH-g-EPDM) on the properties of EPDM nanocomposites reinforced by halloysite nanotubes. *Polym. Test.* **2009**, *28*, 548–559. [CrossRef]
36. Salmah, H.; Ruzaidi, C.M.; Supri, A.G. Compatibilisation of polypropylene/ethylene propylene diene terpolymer/kaolin composites: The effect of maleic anhydride-grafted-polypropylene. *J. Phys. Sci.* **2009**, *20*, 99–107.
37. López Manchado, M.A.; Arroyo, M.; Biagiotti, J.; Kenny, J.M. Enhancement of mechanical properties and interfacial adhesion of PP/EPDM/flax fiber composites using maleic anhydride as a compatibilizer. *J. Appl. Polym. Sci.* **2003**, *90*, 2170–2178. [CrossRef]
38. Barra, G.M.O.; Crespo, J.S.; Bertolino, J.R.; Soldi, V.; Pires, A.T.N. Maleic anhydride grafting on EPDM: Qualitative and quantitative determination. *J. Braz. Chem. Soc.* **1999**, *10*, 31–34. [CrossRef]
39. Jiang, Z.; Du, Z.; Xue, J.; Liu, W.; Li, M.; Tang, T. Hierarchical structure and properties of rigid PVC foam crosslinked by the reaction between anhydride and diisocyanate. *J. Appl. Polym. Sci.* **2018**, *135*, 46141. [CrossRef]
40. Zhou, M.; He, Y.; Chen, Y.; Yang, Y.; Lin, H.; Han, S. Synthesis and evaluation of terpolymers consist of methacrylates with maleic anhydride and methacrylic morpholine and their amine compound as pour point depressants in diesel fuels. *Energy Fuels* **2015**, *29*, 5618–5624. [CrossRef]
41. Yang, N.; Zhang, Z.C.; Ma, N.; Liu, H.L.; Zhan, X.Q.; Li, B.; Gao, W.; Tsai, F.C.; Jiang, T.; Chang, C.J.; et al. Effect of surface modified kaolin on properties of polypropylene grafted maleic anhydride. *Results Phys.* **2017**, *7*, 969–974. [CrossRef]
42. Guo, H.; Meador, M.A.; McCorkle, L.S.; Scheiman, D.A.; McCrone, J.D.; Wilkewitz, B. Poly(maleic anhydride) cross-linked polyimide aerogels: synthesis and properties. *RSC Adv.* **2016**, *6*, 26055–26065. [CrossRef]
43. Chen, J.; Yu, Y.; Chen, J.; Li, H.; Ji, J.; Liu, D. Chemical modification of palygorskite with maleic anhydride modified polypropylene: mechanical properties, morphology, and crystal structure of palygorskite/polypropylene nanocomposites. *Appl. Clay Sci.* **2015**, *115*, 230–237. [CrossRef]

44. Heravi, M.M.; Hashemi, E.; Beheshtiha, Y.S.; Ahmadi, S.; Hosseinnejad, T. $PdCl_2$ on modified poly(styrene-co-maleic anhydride): A highly active and recyclable catalyst for the Suzuki-Miyaura and Sonogashira reactions. *J. Mol. Catal. A Chem.* **2014**, *394*, 74–82. [CrossRef]
45. Kim, J.K.; Park, S.H.; Hyun, T.O.; Jeon, H.K. The effect of weld-lines on the morphology and mechanical properties of amorphous polyamide/poly(ethylene-ran-propylene) blend with various amounts of an in situ compatibilizer. *Polymer* **2001**, *42*, 2209–2221. [CrossRef]
46. Koriyama, H.; Oyama, H.T.; Ougizawa, T.; Inoue, T.; Weber, M.; Koch, E. Studies on the reactive polysulfone-polyamide interface: Interfacial thickness and adhesion. *Polymer* **1999**, *40*, 6381–6393. [CrossRef]
47. Cecchetto, L.; Denoyelle, A.; Delabouglise, D.; Petit, J.P. A silane pre-treatment for improving corrosion resistance performances of emeraldine base-coated aluminium samples in neutral environment. *Appl. Surf. Sci.* **2008**, *254*, 1736–1743. [CrossRef]
48. Van der Wal, A.; Mulder, J.J.; Oderkerk, J.; Gaymans, R.J. Polypropylène-rubber blends: 1. The effect of the matrix properties on the impact behaviour. *Polymer* **1998**, *39*, 6781–6787. [CrossRef]
49. Chatterjee, K.; Naskar, K. Development of thermoplastic elastomers based on maleated ethylene propylene rubber (m-EPM) and polypropylene (PP) by dynamic vulcanization. *Express Polym. Lett.* **2007**, *1*, 527–534. [CrossRef]
50. Loan, L.D. Mechanism of peroxide vulcanization of elastomers. *Rubber Chem. Technol.* **1967**, *40*, 149–176. [CrossRef]
51. Baldwin, F.P.; Borzel, P.; Cohen, C.A.; Makowski, H.S.; Van de Castle, J.F. The influence of residual olefin structure on EPDM vulcanization. *Rubber Chem. Technol.* **1970**, *43*, 522–548. [CrossRef]
52. Plueddemann, E.P. Reminiscing on silane coupling agents. *J. Adhes. Sci. Technol.* **1991**, *5*, 261–277. [CrossRef]
53. Kunst, S.R.; Beltrami, L.V.; Cardoso, H.R.; Santana, J.A.; Sarmento, V.H.; Müller, I.L.; Malfatti, C.D. Characterization of siloxane-poly(methyl methacrylate) hybrid films obtained on a tinplate substrate modified by the addition of organic and inorganic acids. *Mater. Res.* **2015**, *18*, 151–163. [CrossRef]
54. Cui, L.; Paul, D.R. Evaluation of amine functionalized polypropylenes as compatibilizers for polypropylene nanocomposites. *Polymer* **2007**, *48*, 1632–1640. [CrossRef]
55. Song, P.; Yu, Y.; Wu, Q.; Fu, S. Facile fabrication of HDPE-g-MA/nanodiamond nanocomposites via one-step reactive blending. *Nanoscale Res. Lett.* **2012**, *7*, 2–18. [CrossRef]
56. Fina, A.; Tabuani, D.; Peijs, T.; Camino, G. POSS grafting on PPgMA by one-step reactive blending. *Polymer* **2009**, *50*, 218–226. [CrossRef]
57. Perrier, S.; Takolpuckdee, P.; Mars, C.A. Reversible addition—Fragmentation chain transfer polymerization: End group modification for functionalized polymers and chain transfer agent recovery. *Macromolecules* **2005**, *38*, 2033–2036. [CrossRef]